The global chromatin compaction pathway silences transcription during meiotic prophase in *C. elegans*

Mezmur D. Belew[1*], Emilie Chien[1*], and W. Matthew Michael[1#]

[1]Department of Biological Sciences, Molecular and Computational Biology Section, University of Southern California, Los Angeles, CA, 90089

[*]denotes equal contribution
[#]denotes corresponding author (mattm@usc.edu)

Abstract/Summary

While it has been appreciated for decades that prophase-arrested oocytes are transcriptionally silenced, the molecular pathway that promotes silencing has remained elusive. Here, using *C. elegans* as a model system, we demonstrate that the global chromatin compaction (GCC) pathway is responsible for genome silencing in both oocytes and spermatocytes. GCC is mediated by a collaboration between topoisomerase II, condensin II, and the H3K9me pathway. For oocytes, we further demonstrate that GCC is under cell cycle control such that it is activated specifically during diakinesis and prior to oocyte maturation. Previous work had shown that GCC silences gene expression in the primordial germ cells (PGCs) of nutrient-deprived L1 larvae, and we demonstrate here that it is also used during gametogenesis, thus showing that GCC is a versatile, signal-mediated genome silencing system.

Introduction

While much is known about how gene expression is controlled at the level of individual loci, far less is known about how transcription is regulated on a global, or genome-wide, level. Despite this knowledge gap, it is becoming increasingly clear that cells can regulate transcription globally, and furthermore, that genome-wide control is important for proper embryonic and germline development (Nakamura and Seydoux, 2008; Robertson and Lin, 2015). This is particularly true for the nematode *C. elegans*. If one considers germline transcription, from gametogenesis to fertilization and on to embryonic and germline development in the next generation, the nematode germline is capable of at least four distinct occurrences of global repression and activation. In adult hermaphrodite gonads, germ cells are born in the distal tip of the gonad, and then proceed through meiosis in a transcriptionally active state. This transcriptional activity serves two purposes: (1) to produce mRNAs required for the proper development of the oocytes, and (2) to produce mRNAs to load into the fertilized embryos to facilitate early embryogenesis. During meiotic diplotene, as oocytes prepare for maturation, transcription is abruptly and globally silenced (Schisa et al., 2001; Walker et al., 2007). Repression of transcription in oocytes is also observed in other organisms. In *Drosophila melanogaster*, oocytes are developmentally arrested at prophase I and repress transcription between the fifth and eighth stages of oogenesis, just before their re-entry into meiosis. Essential factors needed for oocyte development are loaded onto the oocyte by the neighboring nurse cells (Navarro-Costa et al., 2016). Similarly, in mice, primary follicles that contain prophase I arrested oocytes have been shown to repress transcription just before the resumption of meiosis (Moore et al, 1974; Schultz et al, 2018). This repression persists

throughout fertilization until minor zygotic genome activation (ZGA) occurs at first cleavage (Moore and Lintern-Moore, 1974; Abe et al., 2018). The conservation of this theme across organisms of different complexity suggests that global transcriptional repression in oocytes is an important feature of the oocyte-to-embryo transition. Despite this conservation, however, the molecular pathway(s) responsible for repression are still largely unknown.

In *C. elegans*, transcriptionally silent oocytes are fertilized and transcription remains repressed through the first two mitotic divisions. At the four-cell stage the genome reawakens in the 3 of the 4 cells, all somatic precursors, and remains silenced in the germline precursor (the P_2 cell). Later, at the 100-cell stage, the primordial germ cell (PGC) P_4 divides to form the Z2 and Z3 PGCs, and transcription is activated (Nakamura and Seydoux, 2008; Robertson and Lin, 2015). Z2/Z3 remain transcriptionally active as the embryo hatches; however, if the emerging L1 larvae are placed in an environment lacking food, then Z2/Z3 globally repress transcription (Wong et al, 2018; Belew et al, 2021). Transcriptional repression in Z2/Z3 is mediated by a collaboration between topoisomerase II (TOP-2), the condensin II complex, and components of the heterochromatin pathway, and is coupled to a dramatic compaction of PGC chromatin. Accordingly, we named this new form of genome-wide transcriptional repression the global chromatin compaction (GCC) pathway (Belew et al, 2021).

In this study, we address the problem of how oocytes in *C. elegans* shut down transcription as a function of entering meiotic prophase. The nematode is an ideal system to address this important question, as the events leading up to oocyte maturation and fertilization are well

described. During germline development in hermaphrodites, animals first produce sperm and then switch to making oocytes. Oocytes are produced in an assembly-line like process, where cells exit pachytene and then progress through meiotic prophase within the proximal portion of the tube-shaped gonad. Within the proximal gonad, oocytes can be clearly identified by their position relative to the spermatheca, the oocyte closest is named -1, and the next most proximal oocyte -2, et cetera. Previous work has shown that -4 and -3 oocytes are transcriptionally active, and then the genome is silenced by the -2 position (Walker et al, 2007; see Figure 1A). Other work has shown that, just prior to genome silencing, the condensin II complex is recruited to chromatin, where it helps to compact chromatin during the formation of bivalents, a unique chromosome structure that enables the subsequent meiotic divisions (Chan et al, 2004; see Figure 1A). By the -2 position bivalents have formed and the genome is silenced. At the -1 position the oocyte receives a signal from sperm to initiate maturation, and the cells then enter meiotic M-phase (Figure 1A). Here, we test the hypothesis that our previously described GCC pathway for genome silencing is the mechanism by which oocytes silence transcription, and we find that it is. We also report a requirement for GCC in genome silencing during spermatogenesis. These data supply the first molecular pathway for genome silencing during gametogenesis in any system.

Results

RNAPIIpSer2 is dependent on CDK-9 in proximal oocytes.

The goal of this study was to analyze genome silencing during gametogenesis in *C. elegans*. Accordingly, we initiated our studies by staining oocytes within dissected hermaphrodite gonads using an antibody that recognizes the active and elongating form of RNAPII. This antibody detects a phospho-epitope at the second serine on the carboxy-terminal domain (CTD) of RNAPII (RNAPIIpSer2; Palancade and Bensaude, 2003). Prior work that examined proximal oocytes has shown that RNAPIIpSer2 signals decreased starting with the fourth most proximal oocyte (termed -4) and became undetectable through the two most proximal oocytes (-2 and -1) (Walker et al., 2007). We, therefore, focused our analysis on the four most proximal oocytes and found that RNAPIIpSer2 signal was detected invariably on the chromatin of oocytes at the -4 position (Figure 1B, control RNAi panel). However, as we examined the three most proximal oocytes, we observed several different patterns for the RNAPIIpSer2 signal: (1) signal exclusively on chromatin, (2) no signal at all, (3) signal present both on and off chromatin, and (4) a nucleoplasmic RNAPIIpSer2 signal that mostly excludes chromatin (Figures 1B and 2A). It thus appears that while in some oocytes RNAPIIpSer2 signal completely disappeared, in others, it was merely removed from the chromatin and was present in the nucleoplasm. This form of nucleoplasmic signal has also been observed in human cells as they approach mitosis and is explained by RNAPII coming off the chromatin while maintaining CTD phosphorylations (Hintermair et al, 2016). To confirm that the nucleoplasmic RNAPIIpSer2 signal was due to actual pSer2, and not a cross-reacting epitope, we stained animals that had been exposed to *cdk-9* RNAi, as CDK-9 is one of two kinases responsible for generating pSer2 within RNAPII's CTD

in *C. elegans* (Shim et al, 2002). As shown in Figure 1B, all of the RNAPIIpSer2 signal, both the chromatin and the nucleoplasmic forms, was reduced by the RNAi treatment. This finding makes two important points. First, the data show that the nucleoplasmic RNAPIIpSer2 signal is legitimate and is likely the result of RNAPII that has become disengaged with chromatin. Thus, we only considered nuclei where RNAPIIpSer2 was found on DNA as being transcriptionally active. Second, these data also show that CDK-9 is the major RNAPIISer2 kinase in proximal oocytes. Interestingly, previous work has shown that loss of CDK-9 did not impact RNAPIIpSer2 in the adult *C. elegans* germline, and that CDK-12 is the major RNAPIISer2 kinase in the mitotic and pachytene regions of the gonad (Bowman et al, 2013). We note that this study did not directly examine proximal oocytes. In our *cdk-9* RNAi samples we observed little impact of CDK-9 depletion on RNAPIIpSer2 signals in the pachytene region (Figure 1C), consistent with the work of Bowman and colleagues. It thus appears that there is a handoff, from CDK-12 to CDK-9, for RNAPIIpSer2 during oogenesis in *C. elegans*.

<u>The TOP-2/condensin II axis controls genome silencing during meiotic prophase.</u>

Our data, together with previous findings (Walker et al, 2007), show that genome silencing initiates at the -3 position and is largely complete by the -2 position. We next asked if TOP-2 and/or condensin II was responsible for silencing, as they are during L1 starvation (Belew et al, 2021). For this we examined RNAPIIpSer2 in oocytes from animals exposed to either *top-2, capg-2* (which encodes a protein specific for the condensin II complex), or double *top-2/capg-2* RNAi. All three of these treatments impacted the RNAPIIpSer2 pattern in a similar manner: signal now persisted in -2 oocytes, indicating that genome silencing had failed (Figure 2A&B).

Interestingly, oocytes in the -1 position showed no differences between the control and TOP-2 and/or CAPG-2 depleted samples (Figures 2A and 2B). This is consistent with the fact that -1 oocytes have entered meiotic M-phase, and thus an M-phase specific mechanism for inactivating transcription is in play in these cells (Gottesfeld and Forbes, 1997).

Our data suggest that TOP-2/condensin II are required to silence the genome in -3/-2 oocytes, however the data can also be explained by an indirect effect of slowing down the cell cycle. If loss of TOP-2/condensin II impedes cell cycle progression, it may be that these oocytes are simply delayed in entering prophase, and this is why transcription persists. To examine this possibility, we stained control and *top-2/capg-2* RNAi gonads for the presence of phospho-Serine 10 on histone H3 (H3pS10), a marker for prophase entry (Hendzel et al, 1997). As shown in Figure 3, there was no difference in the timing of the appearance of H3pS10 signals between control and *top-2/capg-2* RNAi samples, showing that progression into prophase is not perturbed by TOP-2/CAPG-2 depletion. Interestingly, in some samples, the intensity of H3pS10 signals appeared to be stronger in *top-2/capg-2* RNAi samples, relative to controls, but this was not always the case. We conclude that the failure to silence transcription in TOP-2/condensin II compromised oocytes is not an indirect effect of delayed entry into prophase.

<u>H3K9me3 marks accumulate on oocyte chromatin during genome silencing.</u>

Our previous work showed that, in starved L1s, genome silencing occurs via collaboration between TOP-2/condensin II and components of the heterochromatin pathway (Belew et al, 2021). Furthermore, the Z2/Z3 PGCs accumulate H3K9me marks to a significant extent, relative

to somatic cells, as they prepare for silencing. Thus, to pursue our studies on genome silencing during oogenesis, we stained oocytes for H3K9me3. We limited the analysis to H3K9me3 because available antibodies against H3K9me2 do not recognize their target when the neighboring serine 10 is phosphorylated (Kimura et al, 2008), and we have seen in Figure 3 that H3pS10 is prominent in proximal oocytes. As shown in Figure 4A, H3K9me3 first appears in -5 oocytes, and then gradually accumulates such that by the -2 and -1 positions the H3K9me3 and DNA signals overlap entirely. To examine the reproducibility of this pattern we developed a scoring scheme for H3K9me3 signal intensity (Figure S1) and applied it across 10 samples. As shown in Figure 4B, the progressive accumulation of H3K9me3, as a function of oocyte position, was highly reproducible. In *C. elegans*, H3K9me3 is produced primarily by the SET-25 methyltransferase (Towbin et al, 2012). Indeed, when H3K9me3 was examined in *set-25* mutants and compared to wild type samples, we observed that the H3K9me signals were attenuated (Figure 4C). No such attenuation was observed when *met-2* mutants were compared to wild type (Figure 4D), consistent with the MET-2 methyltransferase primarily responsible for producing H3K9me1 and me2 (Towbin et al, 2012). We conclude that H3K9me3 marks accumulate dramatically at the time that oocytes are silencing their genomes.

<u>Both the SET-25 and MET-2 methyltransferases are required for genome silencing in oocytes.</u>

Having observed SET-25 dependent accumulation of H3K9me3 marks in proximal oocytes we next asked if SET-25 plays a role in genome silencing. Staining of *set-25* mutants for RNAPIIpSer2 revealed that -2 oocytes contained significantly more active RNAPII than did the control samples (Figure 5A&B), showing that silencing was attenuated. Interestingly, we also

observed a silencing defect in *met-2* mutants (Figure 5A&B). Thus, not only do H3K9me marks accumulate during silencing, but the enzymes responsible for catalyzing these modifications are also important for genome silencing. We conclude that the TOP-2/condensin II axis functions in conjunction with the H3K9me pathway to silence transcription in developing oocytes.

<u>Genome silencing is coupled to global chromatin compaction in oocytes.</u>

Previous work has shown that condensin II loads on to oocyte chromosomes at the -3 position and is required for the intense chromatin compaction that occurs as bivalents are formed (Chan et al, 2004). In starved L1s, genome silencing is coupled to global chromatin compaction (Belew et al, 2021), and thus it was important to monitor compaction in the oocyte system. For this we turned to a previously utilized strain that carries a transgene encoding mCherry-tagged histone H2B, which marks chromatin (Wong et al, 2018; Belew et al, 2021). Living hermaphrodites were immobilized and oocyte chromatin was imaged using confocal microscopy. We compared control samples to those that been exposed to *top-2/capg-2* RNAi, and we looked exclusively at -2 oocytes, which is where bivalent formation is occurring. Superficial inspection of the images revealed that the chromatin masses in the *top-2/capg-2* RNAi samples were larger than control samples (Figure 4A), and this was confirmed by taking measurements along the long axis of the bundles (Figures 4B and S2). The increased size of the bivalents shows that TOP-2 and condensin II are required for compaction, and this is consistent with previous work (Chan et al, 2004). We note that the effects observed here, a modest increase in bivalent size, are less extreme than those reported by Chan and colleagues, and this is likely due to differences in how condensin II was inactivated. In our experiments, we use a feeding RNAi treatment that

targets *capg-2*. By contrast, Chan and colleagues combined RNAi with a temperature-sensitive allele, both targeting the *hcp-6* subunit of condensin II, thereby using two forms of condensin II inactivation in the same experiment. As detailed by Chan and colleagues, the effect on bivalent compaction of the temperature-sensitive *hcp-6* (*hcp-6*^{ts}) allele alone, without RNAi, is rather modest. Given that both the *set-25* and *met-2* methyltransferase mutants show genome silencing defects (Figure 5), we also examined the effects of depleting them on bivalent compaction. As shown in Figures 6A&B, depletion of both methyltransferases led to a significant increase in bivalent size. Taken together, data presented here show that the GCC pathway, first identified in the PGCs of starved L1s, is responsible for genome silencing in oocytes.

<u>The GCC pathway silences the spermatocyte genome during meiotic prophase.</u>

As is the case with oocytes, spermatocytes in *C. elegans* undergo a chromatin compaction event occurring post-pachytene and prior to the onset of the meiotic divisions. It was, therefore, of interest to determine if GCC-mediated genome silencing was occurring in spermatocytes. For this we dissected male gonads and stained for RNAPIIpSer2. We focused our attention on the so-called “compaction zone” (Shakes et al, 2009), which is where developing spermatocytes are positioned after pachytene exit. Nuclei within the compaction zone have a distinct morphology; they are smaller than pachytene nuclei and substantially larger than fully matured spermatids (Figure 7A; L'Hernault, 2006; Shakes et al, 2009). We found that, in wild type males, RNAPIIpSer2 was detected throughout the pachytene region (data not shown), and that the signal was reduced or absent in nuclei at the pachytene/compaction zone boundary, rendering

the remainder of the compaction zone devoid of signal (Figure 7B). By contrast, in samples exposed to *top-2, capg-2,* or *met-2* RNAi, a significantly higher percentage of compaction zone nuclei retained the RNAPIIpSer2 mark (Figures 7C-F). These data show that spermatogenesis represents a third example where the GCC pathway promotes genome silencing, after L1 starvation and oogenesis.

<u>GCC-mediated genome silencing in oocytes is under cell cycle control.</u>

In a final experiment, we were interested in identifying the trigger for GCC within the oocyte system. In the PGCs of starved L1s, a low-energy environment is sensed by AMPK, which then activates GCC for genome shutdown. What is the analogous trigger in oocytes? In mitotic cells, activation of condensin II during prophase requires CDK-dependent phosphorylation of CAPD-3 on threonine 1415 (Abe et al, 2011), a site conserved in the *C. elegans* ortholog (HCP-6). We thus considered the possibility that CDK, via its ability to activate condensin II, would also be the trigger for genome silencing. To explore this possibility, we took advantage of previous work showing that depletion of WEE-1.3, a negative regulator of CDK, hyperactivates CDK in the proximal gonad (Burrows et al, 2006). We thus reasoned that if CDK triggers genome silencing, then hyperactivation of CDK would lead to inappropriate silencing in more distally located oocytes. We again used RNAPIIpSer2 staining to mark transcriptionally active nuclei, and for control samples, the expected pattern emerged where transcription was shut down as oocytes transitioned from the -3 to -2 position (Figure 8). By stark contrast, in the *wee-1.3* RNAi samples, we observed that transcription had been repressed much earlier, such that even some -6 oocytes had shut down gene expression (Figure 8). We note that previous work has shown

that co-depletion of CDK-1 with WEE-1.3 reversed all of the phenotypes observed with WEE-1.3 depletion alone, demonstrating that CDK-1 is the sole target of WEE-1.3 in the hermaphrodite gonad (Burrows et al, 2006). To make sure that the inappropriate transcriptional repression in distal oocytes seen in *wee-1.3* RNAi animals is achieved through the action of CDK on the condensin II complex, we depleted both WEE-1.3 and the condensin II subunit, CAPG-2 and asked if the RNAPIIpSer2 signals were restored. Indeed, upon *wee-1.3/capg-2* RNAi treatment, we saw that the disbursement of RNAPIIpSer2 signal within proximal oocytes now matched the wild type pattern (Figure 8). Thus, we conclude that genome silencing is under cell cycle control and that it is likely that CDK itself is the trigger, via activation of condensin II.

Discussion

In this work we tested the hypothesis that transcriptional repression in prophase oocytes is controlled by our previously described GCC pathway and found that it is. In support of this conclusion, we showed that depletion of the GCC components TOP-2, CAPG-2 (of condensin II), MET-2, and SET-25 all result in the persistence of active RNAPII in -2 oocytes and a defect in chromatin compaction (Figures 2, 5, and 6). These results are similar in nature to what we reported for the Z2/Z3 PGCs during starvation; in both systems we see a massive buildup of H3K9me marks, leading to chromatin compaction and genome silencing. In work reported here we provide evidence that GCC is also required for transcriptional repression during spermatogenesis. Thus, GCC is responsible for the global repression of transcription in at least three distinct developmental contexts in the *C. elegans* germline.

Transcriptional repression during oogenesis is a universally conserved process yet we know very little about the factors responsible for repression. The work presented here shows that the GCC pathway controls silencing in *C. elegans*, but what is known in other systems? In mice, it has been appreciated for some time that oocytes undergo chromatin compaction concurrent with transcriptional repression (Zuccotti et al, 1995; Bouniol-Baly et al, 1999; De La Fuente et al., 2004; Schultz et al, 2018). Interestingly, very recent work has shown that a histone H3.3 chaperone complex, comprised of the Hira and Cabin1 proteins, promotes H3K9me3 deposition in chromatin, chromatin compaction, and genome silencing in mouse oocytes (Smith et al, 2022). These data are consistent with our findings with the GCC pathway and suggest that a conserved feature of genome silencing is the H3K9me-mediated compaction of chromatin on a

global scale. It will be of interest to determine if TOP-2 and/or condensin II are also required for genome silencing in murine oocytes.

One important question that arises from our studies becomes: how is genome silencing regulated during germline development? Clearly it must happen at the proper time, otherwise development would suffer. In the Z2/Z3 PGCs we have seen that H3K9me marks accumulate to a dramatic extent in late embryos, however these nuclei are still transcriptionally active (Belew et al, 2021). Chromatin compaction in late embryos occurs, but the compaction is not as extreme as it will be in a starved L1, and it is only during L1 starvation that Z2/Z3 compact the chromatin to an extent that transcription is repressed. Thus, for Z2/Z3, it appears that during late embryogenesis the nuclei are preparing for the possibility of a genome shutdown, via the accumulation of H3K9me marks, but the trigger is not squeezed until AMPK is activated by low energy in a starved L1. Our current work reveals a different regulatory strategy for oocytes. In the oocyte system it appears that H3K9me accumulation is concurrent with genome silencing, such that by the -2 position H3K9me signals are peaking while RNAPIIpSer2 signals are largely extinguished. One important difference between Z2/Z3 and oocytes is that Z2/Z3 silence transcription in response to an environmental condition, one that is not always a concern, whereas silencing in oocytes is a constitutive event. Since condensin II activation requires CDK (Abe et al, 2011), we hypothesized that silencing would be under cell cycle control. Consistent with this, when we accelerated cell cycle progression, via depletion of the CDK regulator WEE-1.3, we observed that silencing was also accelerated (Figure 8). We propose that CDK is tightly controlled during meiotic prophase, such that its activity gradually rises as the system

progresses through diplotene and diakinesis. As CDK levels rise above a threshold at the -3 position, condensin II is abruptly activated and loaded onto chromatin, and compaction and silencing are then triggered. We note that this threshold of CDK activity is below that required to trigger meiotic M-phase, as the nuclear envelope remains intact during genome silencing. Consistent with this notion, in human HeLa cells it has been clearly shown that CyclinB1-CDK1 is progressively activated during prophase (Gavet and Pines, 2010). How might CDK activity be so finely tuned in the gonad? It may be that extracellular signals, produced by the somatic gonad in a positionally controlled manner, modulate CDK such that its activity gradually rises as oocytes move toward the spermatheca. While there is precedent for soma-germline communication to control CDK at maturation (Huelgas-Morales and Greenstein, 2018), to our knowledge such regulation at more distal positions has not been described.

Finally, it is worth considering how GCC-mediated genome silencing is occurring mechanistically. In mammals, resting T-cells contain highly compacted chromatin that prevents transcriptional activators such as Stat5 from gaining access to DNA (Rawlings et al, 2011). Compaction depends on condensin II, and the compacted state is rapidly reversed upon T-cell activation, such that Stat5 can now gain access to target promoters. These data imply a steric hindrance-based mechanism that physically shields promoters from occupancy by transcription factors. How might this be happening at the level of genome architecture? Work on quiescent budding yeast cells has shown that global transcriptional repression is mediated by condensin by organizing chromatin into so-called large chromosomal interaction domains (L-CIDs; Swygert et al, 2019). L-CIDs are thought to form via condensin-mediated loop extrusion, with the loops

averaging ~13 kb in size. Loop extrusion is controlled by condensin's interaction with the transcription machinery at promoters, and thus repression is thought to occur in two ways; first by condensin binding at promoters to prevent their activation, and second by chromatin within the loop interacting in a manner that prevents transcription factor access. One important difference between these examples and the GCC pathway in worms is the requirement for H3K9me in GCC. One exciting possibility is that, for GCC, condensin also mediates loop extrusion, and the role of H3K9me and its conjugate reader proteins is to drive interactions within the loop in a manner that blocks promoter access by transcription factors. Having identified a role for GCC in genome silencing in three different contexts, the next wave of research will focus on mechanism, and such experiments are now in progress.

Materials and Methods

C. elegans strains

N2 (wild-type), WMM1 ([pie-1::gfp::pgl-1 + unc-119(+)]; [(pAA64)pie-1p::mCherry::his-58 + unc-119(+)] IV), MT13293(met-2(n4256) III), MT17463 (set-25(n5021) III) strains were used in this study. Worms were maintained on 60mm plates containing nematode growth media (NGM) seeded with the *E. coli* strain OP50 or HT115. Worms were grown at 20°C and propagated through egg preparation (bleaching) every 72 hours.

Bacterial strains

OP50 bacteria served as the primary food source. It was grown in LB media containing 100 ug/ml streptomycin by shaking at 37°C overnight. 500 ul of the culture was seeded on Petri-dishes containing NGM + streptomycin. HT115 bacteria grown in LB media containing 100 ug/ml carbenicillin and 12.5 ug/ml tetracycline and seeded on NGM + carbenicillin + tetracycline plates were also used as a source of food. Our RNAi strains were obtained from the Ahringer library and verified by Sanger sequencing. Bacteria containing dsRNA were streaked on LB-agar plates containing 100 ug/ml carbenicillin and 12.5 ug/ml tetracycline and incubated at 37°C overnight. Single colonies were then picked and grown in 25ml LB cultures with 100 ug/ml carbenicillin and 12.5 ug/ml tetracycline. 500 ul of this culture was seeded on 60 mm Petri-dishes containing 5mM IPTG.

Egg preparation

Bleach solution containing 3.675 ml H2O, 1.2 NaOCl, and 0.125 ml 10N NaOH was prepared. Adult worms were washed from plates with 5 ml of M9 minimal medium (22mM KH2PO4, 22mM Na2HPO4, 85mM NaCl, and 2mM MgSO4). Worms were centrifuged at 1.9 KRPM for 1 minute and the excess medium was removed, then the bleach solution was added. Eggs were extracted by vortexing for 30 seconds and shaking for 1 minute. This was done a total of 3 times and worms were vortexed one last time. Then the eggs were spun down at 1900 rpm for 1 minute and excess bleach solution was removed and the eggs were washed 3 times with M9 minimal medium.

RNAi treatment

RNAi containing NGM plates were prepared as described in the "Bacterial strains" section. For double RNAi treatments, RNAi cultures were mixed at a 1:1 ratio by volume. HT115 cells transformed with an empty pL4440 vector was used as a negative control. RNAi conditions used in this study and tests for their efficacy is described below:

<u>*cdk-9* RNAi</u>

L1 worms were plated on HT115 food plates for the first 48 hours and were then moved to plates containing *cdk-9* RNAi for the remaining 24 hours. Embryonic lethality in the range of 80% - 85% was observed.

<u>*top-2* RNAi</u>

L1 worms were plated on HT115 food plates for the first 24 hours and were then moved to plates seeded with *top-2* RNAi for the remaining 48 hours. Embryonic lethality was observed at >90%.

capg-2 RNAi

Worms were grown on HT115 food plates for the first 24 hours and were moved to plates containing *capg-2* RNAi for the remaining 48 hours. An embryonic lethality of 80%-100% was seen with this RNAi treatment.

top-2/capg-2 double RNAi

Worms were grown on HT115 food plates for the first 24 hours and were transferred to *top-2/capg-2* double RNAi plates for the next 48 hours. Embryonic lethality ranged from 90%-100% for this RNAi treatment.

met-2 RNAi

Worms were grown on plates containing *met-2* RNAi for the entirety of their life cycle. Some of the adult worms were bleached and an L1 chromatin compaction assay was performed on the resulting larvae to test RNAi efficacy. Please see Belew et al., 2021, for details on the L1 compaction assay.

set-25 RNAi

Worms were grown on plates containing *set-25* RNAi for the entirety of their life cycle. RNAi efficacy was tested as for *met-2* RNAi.

wee-1.3 RNAi

Worms were grown on plates containing *wee-1.3* RNAi for the entirety of their life cycle. An embryonic lethality of ~40% was observed. Additionally, a significant reduction in brood size, and the coalescence of bivalents into one chromatin mass in proximal oocytes of some samples, were observed for *wee-1.3* RNAi worms, as previously reported (Burrows et al., 2006).

wee-1.3/capg-2 double RNAi

Worms were grown on plates containing *wee-1.3* RNAi for 24 hours then were moved to plates containing *wee-1.3/capg-2* RNAi where they remained for the rest of their life cycle. An embryonic lethality of ~80%, and the coalescence of bivalents in proximal oocytes of some samples were observed.

Antibodies and dilutions

RNAPIIpSer2: Rabbit antibody from Abcam (ab5095, Cambridge, Massachusetts) was used at a dilution of 1:100. H3pSer10: Rabbit antibody from Rockland Immunochemicals (600-401-I74, Pottstown, Pennsylvania) was used at a dilution of 1:500. H3K9me3: Rabbit antibody from Abcam (ab176916, Cambridge, Massachusetts) was used at a dilution of 1:1000. Secondary antibodies: Alexa Fluor conjugated secondary antibodies from Invitrogen (Thermofisher Scientific, Waltham, Massachusetts) were used at a dilution of 1:200.

Immunofluorescence staining

Adult worms were first washed off plates with 10 ml of M9 minimal medium and washed 3 more times. Then, they were centrifuged at 1.9 KRPM and the excess medium was removed. 20 ul of media containing about 50 worms were spotted on a coverslip and 3 ul of anesthetic (20mM Sodium Azide and 0.8M Tetramisole hydrochloride) was added to immobilize them. Worms were dissected using 25Gx5/8 needles (Sigma Aldrich, St. Louis, Missouri). To release gonads, adult worms were cut twice, once right below their pharyngeal bulb and once near the tail. The coverslip was then mounted onto poly-L-lysine covered slides and let rest for 5

minutes. Slides were put on dry ice for 30 minutes. Samples were then freeze-cracked by flicking the coverslips off for permeabilization.

For RNAPIIpSer2 and H3pSer10 staining experiments, once samples are permeabilized, slides were put in cold 100% methanol for 2 minutes and then fixing solution (0.08M HEPES pH 6.9, 1.6mM MgSO4, 0.8mM EGTA, 3.7% formaldehyde, 1X phosphate-buffered saline) for another 30 minutes. After fixing, slides were washed three times with TBS-T (TBS with 0.1% Tween-20) and were blocked for 30 minutes with TNB (containing 100mM Tris-HCl, 200 mM NaCl, and 1% BSA). Primary antibodies were then applied at the dilutions described above in TNB and slides were incubated at 4°C overnight.

For H3K9me3 staining experiments, permeabilized samples were put in cold 100% methanol for 10 seconds and then fixing solution (0.08M HEPES pH 6.9, 1.6mM MgSO4, 0.8mM EGTA, 3.7% formaldehyde, 1X phosphate-buffered saline) for 10 minutes. After fixing, slides were washed three times with TBS-T (TBS with 0.1% Tween-20) and were blocked for 2 hours with TNB (containing 100mM Tris-HCl, 200 mM NaCl, and 1% BSA) supplemented with 10% goat serum. Primary antibodies were then applied at the dilutions described above in TNB and slides were incubated at 4°C overnight.

On the next day, the slides were washed 3 times with TBS and slides were incubated with secondary antibodies and Hoechst 33342 dye for 2 hours at room temperature. Slides were washed 3 times with TBS, mounting medium (50 % glycerol in PBS), and coverslips were applied and sealed with Cytoseal XYL (Thermofisher).

Live animal imaging

Adult worms were collected off plates and were washed 3 times with 10 ml M9 minimal medium. After the last wash, worms were spun down at 1.9 KRPM and excess medium was removed. 0.3% agarose pads were made on slides, and a ~5 µl aliquot of adult worms was mounted. A similar volume of anesthetic (20mM Sodium Azide and 0.8M Tetramisole hydrochloride) was added to stop the worms from moving. Then, coverslip was gently applied, and the slides were imaged.

Immunofluorescent imaging

All slides were imaged using an Olympus Fluoview FV1000 confocal microscope using Fluoview Viewer software. Laser intensity was controlled for experiments to achieve consistency among samples.

Statistical analysis

Prior to performing any statistical test, data was tested whether it was parametric or not. To do so, the Shapiro-Wilk test was used to test for normal distribution and F-test was used to test for variance homogeneity of the datasets we were comparing. Data were, then, analyzed using a student's t-test or Wilcoxon Rank Sum test depending on whether the datasets fulfill the requirements for a parametric test or not. Differences between any two datasets were considered statistically significant if a P-value of <0.05 was obtained.

Funding

This work was funded by a grant from the National Institutes of Health (R01GM127477) to W.M.M.

Author Contributions

W.M.M. acquired funding and conceptualized the project. W.M.M designed experiments. M.D.B., E.C., M.M.W., and W.M.M. performed experiments. W.M.M. and M.D.B., and E.C. wrote the manuscript.

Declaration of interests

The authors declare no competing intere

References

1. Abe KI, Funaya S, Tsukioka D, Kawamura M, Suzuki Y, Suzuki MG, Schultz RM, Aoki F. (2018). Minor zygotic gene activation is essential for mouse preimplantation development. Proc Natl Acad Sci U S A. 115(29):E6780-E6788.
2. Abe S, Nagasaka K, Hirayama Y, Kozuka-Hata H, Oyama M, Aoyagi Y, Obuse C, Hirota T. (2011). The initial phase of chromosome condensation requires Cdk1-mediated phosphorylation of the CAP-D3 subunit of condensin II. Genes Dev. 25(8):863-74.
3. Belew MD, Chien E, Wong M, Michael WM. (2021). A global chromatin compaction pathway that represses germline gene expression during starvation. J Cell Biol. 220(9):e202009197.
4. Bouniol-Baly C, Hamraoui L, Guibert J, Beaujean N, Szöllösi MS, Debey P. (1999). Differential transcriptional activity associated with chromatin configuration in fully grown mouse germinal vesicle oocytes. Biol Reprod. 60(3):580-7.
5. Bowman EA, Bowman CR, Ahn JH, Kelly WG. (2013). Phosphorylation of RNA polymerase II is independent of P-TEFb in the C. elegans germline. Development. 140(17):3703-13.
6. Burrows AE, Sceurman BK, Kosinski ME, Richie CT, Sadler PL, Schumacher JM, Golden A. (2006). The C. elegans Myt1 ortholog is required for the proper timing of oocyte maturation. Development. 133(4):697-709.
7. Chan RC, Severson AF, Meyer BJ. (2004). Condensin restructures chromosomes in preparation for meiotic divisions. J Cell Biol. 167(4):613-25.
8. De La Fuente R, Viveiros MM, Burns KH, Adashi EY, Matzuk MM, Eppig JJ. (2004). Major chromatin remodeling in the germinal vesicle (GV) of mammalian oocytes is dispensable

for global transcriptional silencing but required for centromeric heterochromatin function. Dev Biol. 275(2):447-58.

9. Gavet O, Pines J. (2010). Progressive activation of CyclinB1-Cdk1 coordinates entry to mitosis. Dev Cell. 18(4):533-43.
10. Gottesfeld JM, Forbes DJ. (1997). Mitotic repression of the transcriptional machinery. Trends Biochem Sci. 22(6):197-202.
11. Hendzel MJ, Wei Y, Mancini MA, Van Hooser A, Ranalli T, Brinkley BR, Bazett-Jones DP, Allis CD. (1997). Mitosis-specific phosphorylation of histone H3 initiates primarily within pericentromeric heterochromatin during G2 and spreads in an ordered fashion coincident with mitotic chromosome condensation. Chromosoma. 106(6):348-60.
12. Hintermair C, Voß K, Forné I, Heidemann M, Flatley A, Kremmer E, Imhof A, Eick D. (2016). Specific threonine-4 phosphorylation and function of RNA polymerase II CTD during M phase progression. Sci Rep. 6:27401.
13. Huelgas-Morales G, Greenstein D. (2018). Control of oocyte meiotic maturation in C. elegans. Semin Cell Dev Biol. 84:90-99.
14. Kimura H, Hayashi-Takanaka Y, Goto Y, Takizawa N, Nozaki N. (2008). The organization of histone H3 modifications as revealed by a panel of specific monoclonal antibodies. Cell Struct Funct. 33(1):61-73.
15. L'Hernault SW. (2006). Spermatogenesis. WormBook. 1-14. doi: 10.1895/wormbook.1.85.1.
16. Moore GP, Lintern-Moore S. (1974). A correlation between growth and RNA synthesis in the mouse oocyte. J Reprod Fertil. 39(1):163-6.

17. Moore GP, Lintern-Moore S, Peters H, Faber M. (1974). RNA synthesis in the mouse oocyte. J Cell Biol. 60(2):416-22.

18. Nakamura A, Seydoux G. (2008). Less is more: specification of the germline by transcriptional repression. Development.135(23):3817-27.

19. Navarro-Costa P, McCarthy A, Prudêncio P, Greer C, Guilgur LG, Becker JD, Secombe J, Rangan P, Martinho RG. (2016). Early programming of the oocyte epigenome temporally controls late prophase I transcription and chromatin remodelling. Nat Commun. 7:12331.

20. Palancade B, Bensaude O. (2003). Investigating RNA polymerase II carboxyl-terminal domain (CTD) phosphorylation. Eur J Biochem. 270(19):3859-70.

21. Rawlings JS, Gatzka M, Thomas PG, Ihle JN. (2011). Chromatin condensation via the condensin II complex is required for peripheral T-cell quiescence. EMBO J. 30(2):263-76.

22. Robertson S, Lin R. (2015). The Maternal-to-Zygotic Transition in C. elegans. Curr Top Dev Biol. 113:1-42.

23. Schisa JA, Pitt JN, Priess JR. (2001). Analysis of RNA associated with P granules in germ cells of C. elegans adults. Development. 128(8):1287-98.

24. Schultz RM, Stein P, Svoboda P. (2018). The oocyte-to-embryo transition in mouse: past, present, and future. Biol Reprod. 99(1):160-174.

25. Shakes DC, Wu JC, Sadler PL, Laprade K, Moore LL, Noritake A, Chu DS. (2009). Spermatogenesis-specific features of the meiotic program in *Caenorhabditis elegans*. PLoS Genet. 5(8):e1000611.

26. Shim EY, Walker AK, Shi Y, Blackwell TK. (2002). CDK-9/cyclin T (P-TEFb) is required in two postinitiation pathways for transcription in the C. elegans embryo. Genes Dev. 16(16):2135-46.

27. Smith R, Susor A, Ming H, Tait J, Conti M, Jiang Z, Lin CJ. (2022). The H3.3 chaperone Hira complex orchestrates oocyte developmental competence. Development. 149(5):dev200044.

28. Swygert SG, Kim S, Wu X, Fu T, Hsieh TH, Rando OJ, Eisenman RN, Shendure J, McKnight JN, Tsukiyama T. (2019). Condensin-Dependent Chromatin Compaction Represses Transcription Globally during Quiescence. Mol Cell. 73(3):533-546.

29. Towbin BD, González-Aguilera C, Sack R, Gaidatzis D, Kalck V, Meister P, Askjaer P, Gasser SM. (2012). Step-wise methylation of histone H3K9 positions heterochromatin at the nuclear periphery. Cell. 150(5):934-47.

30. Walker AK, Boag PR, Blackwell TK. (2007). Transcription reactivation steps stimulated by oocyte maturation in C. elegans. Dev Biol. 304(1):382-93.

31. Wong MM, Belew MD, Kwieraga A, Nhan JD, Michael WM. (2018). Programmed DNA Breaks Activate the Germline Genome in *Caenorhabditis elegans*. Dev Cell. 46(3):302-315.

32. Zuccotti M, Piccinelli A, Giorgi Rossi P, Garagna S, Redi CA. (1995). Chromatin organization during mouse oocyte growth. Mol Reprod Dev. 41(4):479-85.

Figures and figure Legends

Figure 1

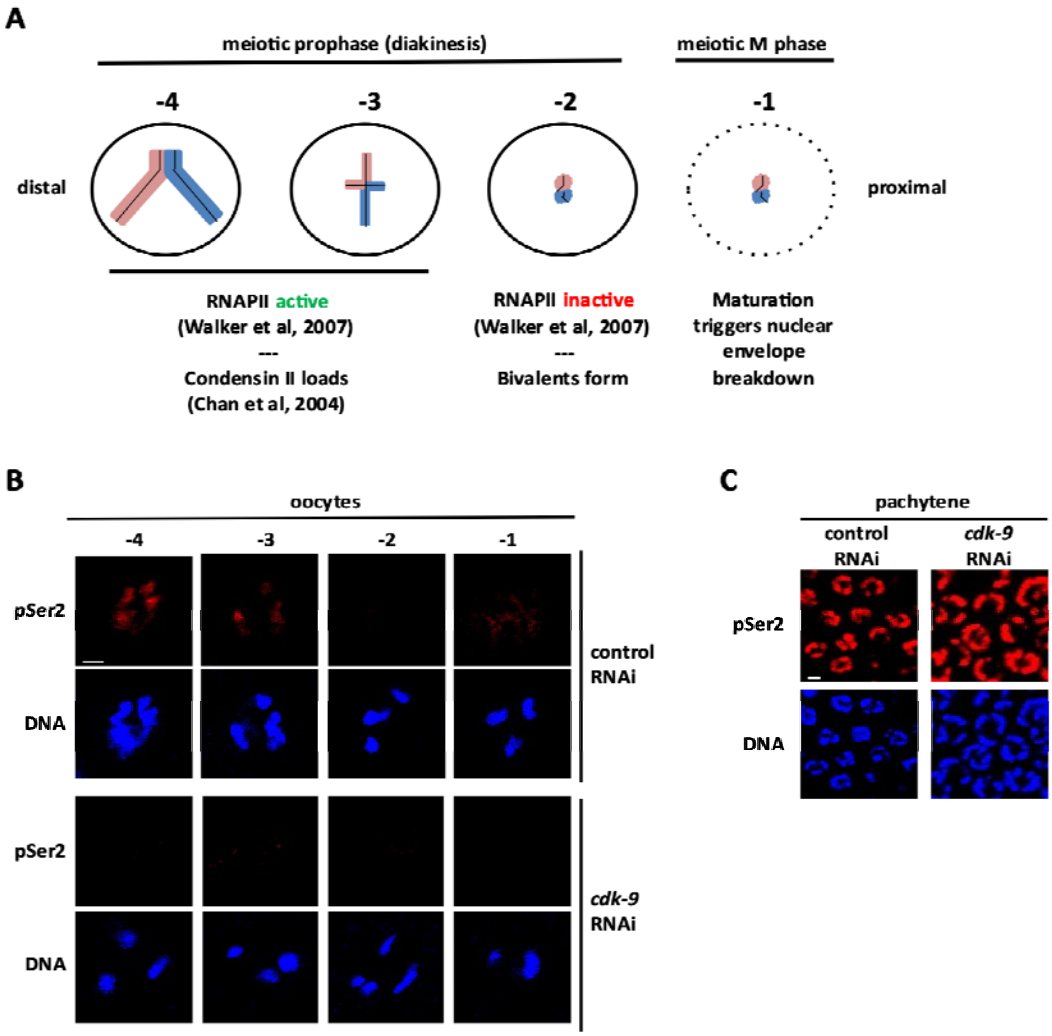

Figure 1: Timing and CDK-9 dependence of the phosphorylation of RNAPIISer2 in *C. elegans* proximal oocytes.

A. Schematic summarizing transcriptional activity and chromatin compaction in the four most proximal oocytes. See introduction for details.

B. N2s were treated with either control or *cdk-9* RNAi. Dissected gonads from these animals were fixed and stained for DNA (blue) and RNAPIIpSer2 (red). Depletion of CDK-9 results in the loss of RNAPIIpSer2 signal in proximal oocytes. Scale bar represents a length of 2 um.

C. Pachytene nuclei from the same animals in (B) were fixed and stained for DNA (blue) and RNAPIIpSer2 (red). Unlike proximal oocytes *cdk-9* RNAi does not alter RNAPIIpSer2 signal in pachytene nuclei. Scale bar represents a length of 2 um.

Figure 2

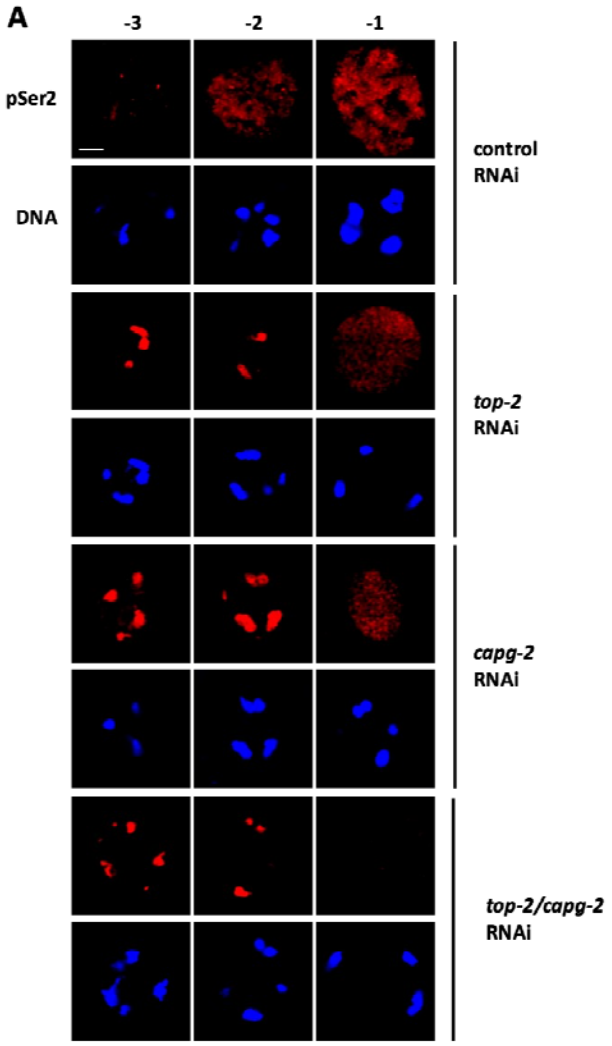
A
-3
-2
-1
pSer2
DNA
control RNAi
top-2 RNAi
capg-2 RNAi
top-2/capg-2 RNAi

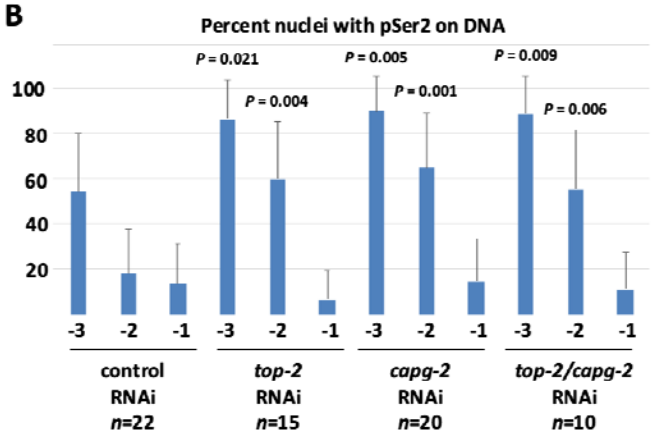
B
Percent nuclei with pSer2 on DNA
P = 0.021
P = 0.004
P = 0.005
P = 0.001
P = 0.009
P = 0.006
100
80
60
40
20
-3 -2 -1 -3 -2 -1 -3 -2 -1 -3 -2 -1
control RNAi n=22
top-2 RNAi n=15
capg-2 RNAi n=20
top-2/capg-2 RNAi n=10

Figure 2: Aberrant RNAPIIpSer2 signal is observed in proximal oocytes when TOP-2 and condensin II are depleted.

A. N2 animals were treated with control, *top-2*, *capg-2,* or *top-2/capg-2* double RNAi. Gonads were dissected from these animals and were fixed and stained for DNA (blue) and RNAPIIpSer2 (red). Representative images for the three most proximal oocytes are shown. Individual depletion of TOP-2 and CAPG-2 and their co-depletion using double RNAi treatment results in persistent RNAPIIpSer2 signal on the chromatin of -3 and -2 oocytes. Scale bar represents a length of 2 um.

B. Quantification of data presented in (A). Percentage of RNAPIIpSer2 positive samples are presented for each oocyte position. Error bars represent one standard deviation. Students T-test was used to obtain P-values.

Figure 3

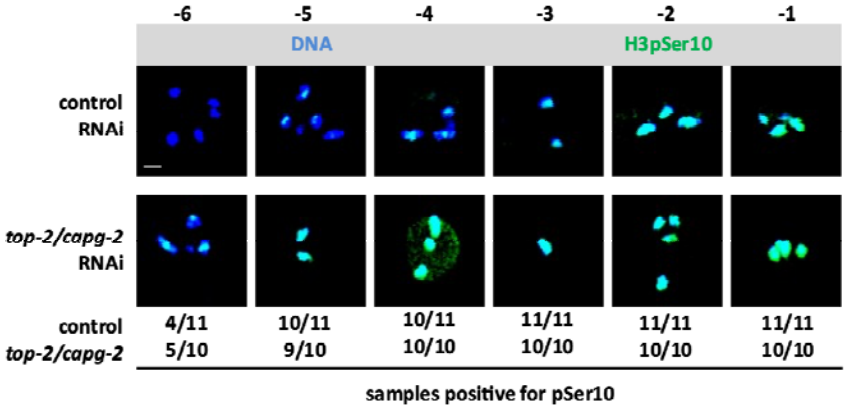
-6
-5
-4
-3
-2
-1
DNA
H3pSer10
control RNAi
top-2/capg-2 RNAi
control
top-2/capg-2
4/11
5/10
10/11
9/10
10/11
10/10
11/11
10/10
11/11
10/10
11/11
10/10
samples positive for pSer10

Figure 3: TOP-2 and condensin II mediated transcriptional repression in oocytes is independent of cell-cycle timing.

N2 animals were treated with control or *top-2/capg-2* double RNAi. Gonads from young adults were dissected and fixed and stained for DNA (blue) and H3pSer10 (green). H3pSer10 signal is quantified below each panel. Exposure to *top-2/capg-2* RNAi does not affect the timing of H3pSer10, and thus does not alter cell cycle progression. Scale bar represents a length of 2 um.

Figure 4

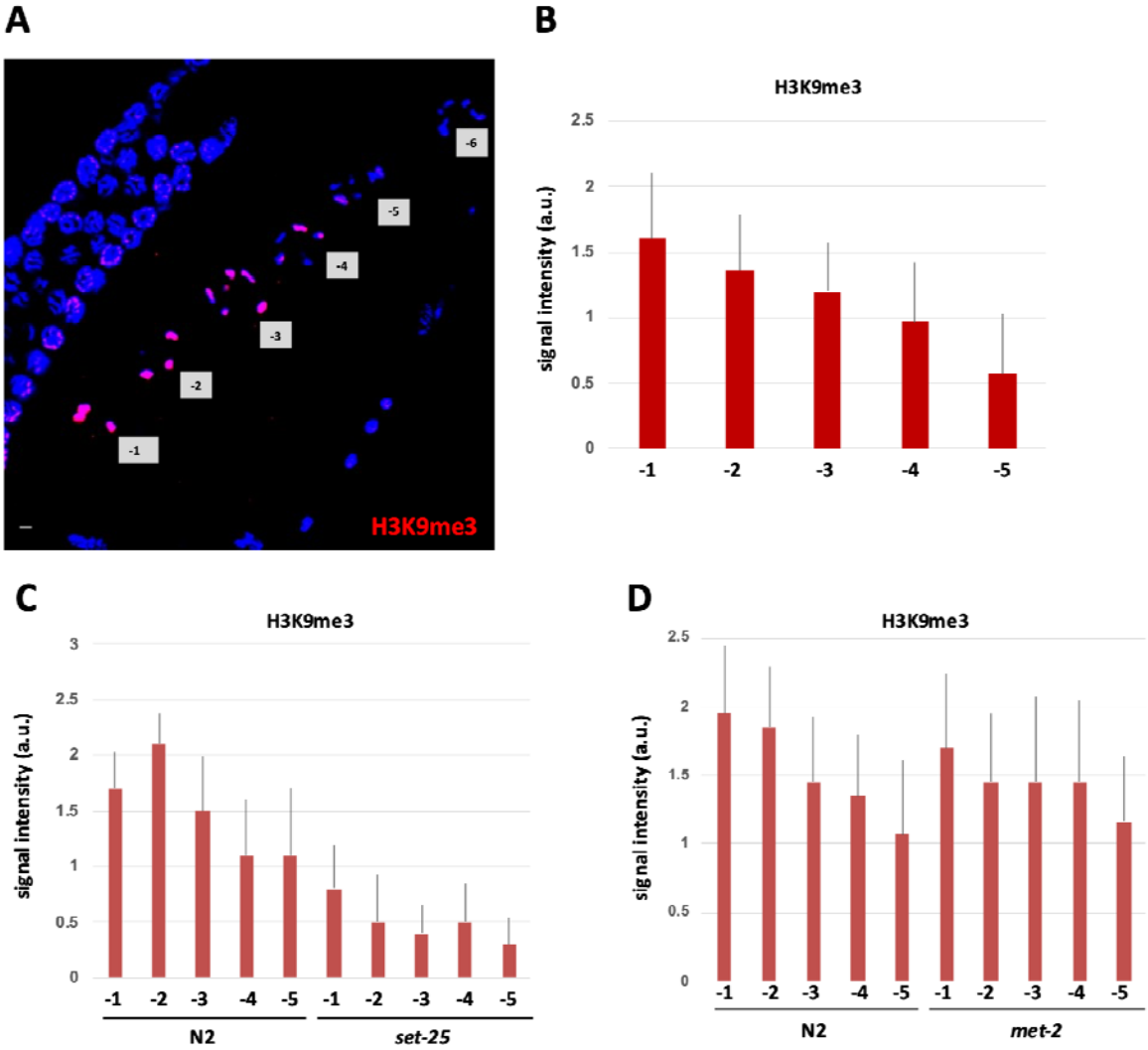
A
-6
-5
-4
-3
-2
-1
H3K9me3
B
H3K9me3
signal intensity (a.u.)
2.5
2
1.5
1
0.5
0
-1
-2
-3
-4
-5
C
H3K9me3
signal intensity (a.u.)
3
2.5
2
1.5
1
0.5
0
-1 -2 -3 -4 -5 -1 -2 -3 -4 -5
N2
set-25
D
H3K9me3
signal intensity (a.u.)
2.5
2
1.5
1
0.5
0
-1 -2 -3 -4 -5 -1 -2 -3 -4 -5
N2
met-2

Figure 4: H3K9me3 signals significantly increase as oocytes become more proximal.

A. Gonads from N2 animals were dissected and stained for DNA (blue) and H3K9me3 (red). Representative image is shown. A marked increase in H3K9me3 signal is observed at the -3 to -1 positions in comparison to more distal oocytes and pachytene nuclei from the same animal. Scale bar represents a length of 2 um.

B. Quantification of data presented in (A). H3K9me3 signals were given a score ranging from 0 to 3, based on signal intensity. Error bars represent 1 standard deviation.

C. Gonads were dissected from wild-type or MT17463 (set-25 mutant) animals. Samples were then fixed, and stained for DNA and H3K9me3. H3K9me3 signals were quantified as in (B) and are presented here. Error bars represent 1 standard deviation. The depletion of SET-25 results in the lowered intensity of H3K9me3 signals.

D. Gonads were dissected from wild-type or MT13293 (*met-2* mutant) animals. Samples were then fixed, and stained for DNA and H3K9me3. H3K9me3 signals were quantified as in (B) and are presented here. Error bars represent 1 standard deviation. *met-2* RNAi treatment does not have any significant effect on the intensity of H3K9me3 signals.

Figure S1

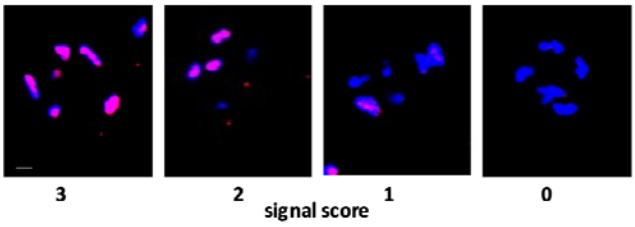

Figure S1: Scoring scheme for H3K9me3 signals used in Figure 4.

Gonads from N2 animals were fixed and stained for DNA (blue) and H3K9me3 (red). Example images of oocytes for each H3K9me signal score from 0 to 3 are shown below. Scale bar represents a length of 2 um.

Figure 5

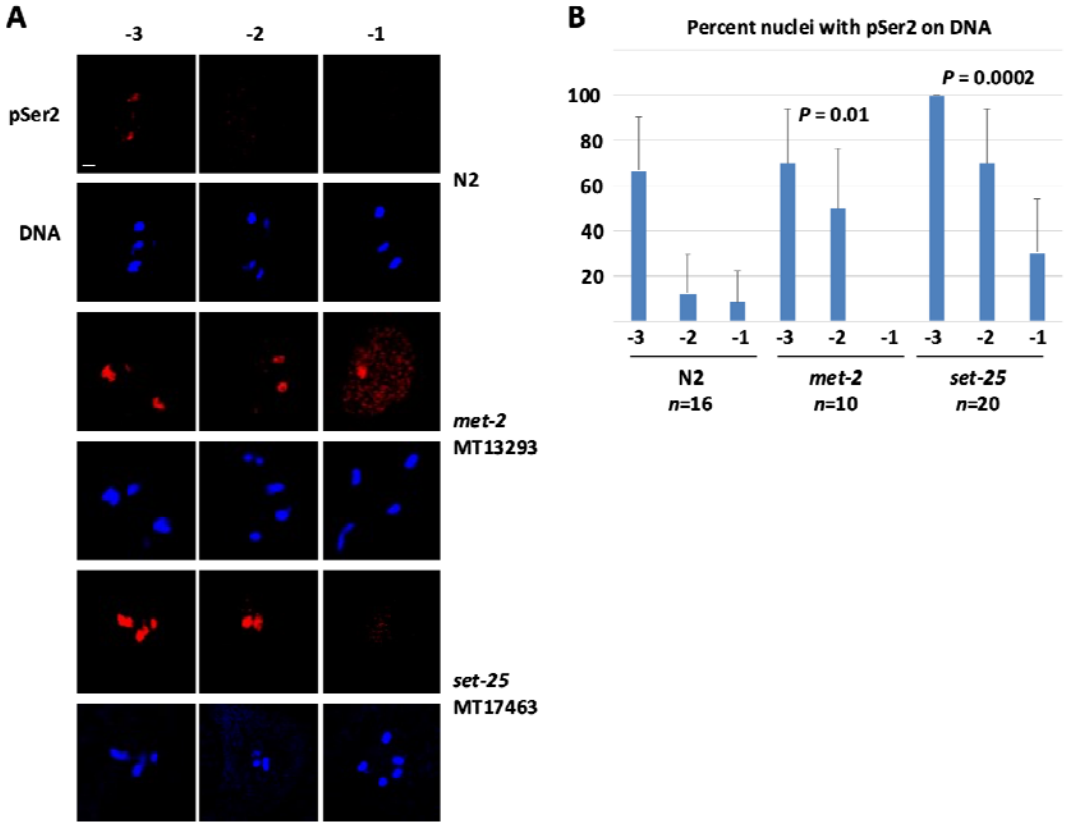
A
-3
-2
-1
pSer2
DNA
N2
met-2
MT13293
set-25
MT17463
B
Percent nuclei with pSer2 on DNA
P = 0.0002
P = 0.01
100
80
60
40
20
-3
-2
-1
-3
-2
-1
-3
-2
-1
N2
n=16
met-2
n=10
set-25
n=20

Figure 5: The H3k9 methyltransferases MET-2 and SET-25 are required for transcriptional repression in proximal oocytes.

A. Gonads from wild-type, *met-2* mutant, and *set-25* mutant animals were dissected. Gonads were then fixed and stained for DNA (blue) and RNAPIIpSer2 (red). Representative images of the three most proximal oocytes are presented. Loss of either *met-2* or *set-25* results in persistent RNAPIIpSer2 signal on chromatin, compared to wild-type animals. Scale bar represents a length of 2 um.

B. Quantification of data presented in (A). Percentage of oocytes with RNAPIIpSer2 signal is presented. Error bars represent one standard deviation. Student's T-test was used to obtain P-values.

Figure 6

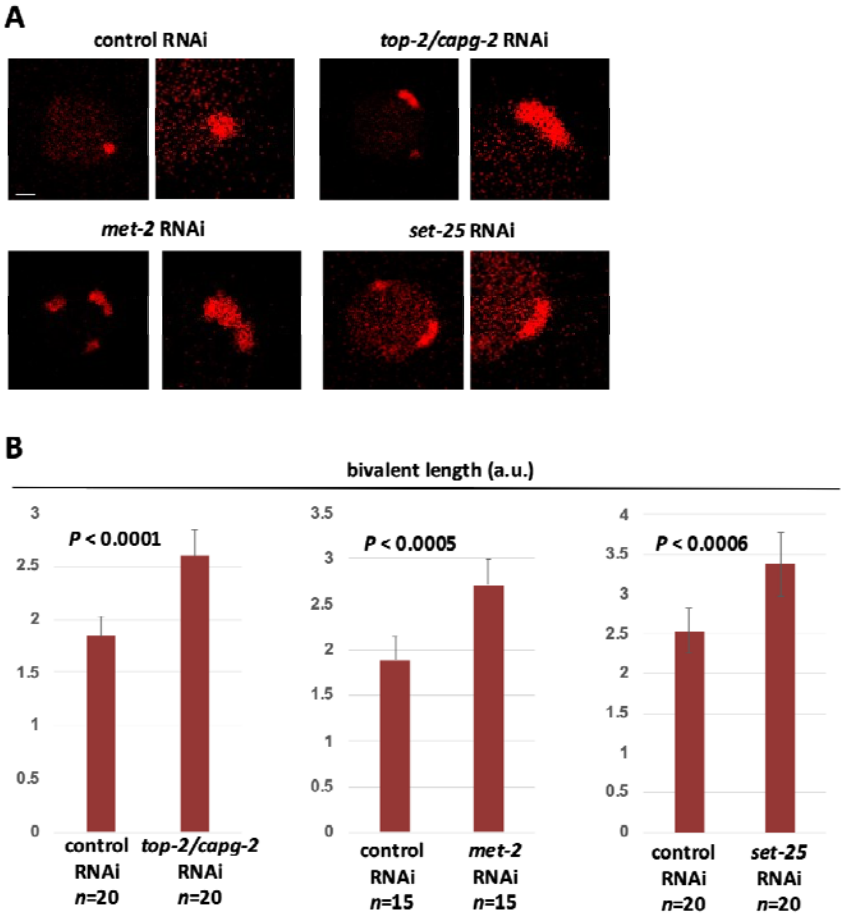
A
control RNAi
top-2/capg-2 RNAi
met-2 RNAi
set-25 RNAi
B
bivalent length (a.u.)
P < 0.0001
control RNAi n=20
top-2/capg-2 RNAi n=20
P < 0.0005
control RNAi n=15
met-2 RNAi n=15
P < 0.0006
control RNAi n=20
set-25 RNAi n=20

Figure 6: TOP-2, condensin II and the H3K9 methyltransferases MET-2 and SET-25 are all required for proper bivalent compaction.

A. Living proximal oocytes, treated with control, *top-2/capg-2*, *met-2,* and *set-25* RNAi, were imaged for chromatin compaction using a strain harboring mCherry-tagged histone H2B. Representative images of oocytes at the -2 position are shown. Exposure to *top-2/capg-2, met-2* or *set-25* RNAi treatments results in significantly larger bivalents in -2 oocytes. Scale bar represents a length of 2 um.

B. Quantification of data presented in (A). Average lengths of bivalents are presented. Error bars represent one standard deviation. Student's T-test or Wilcoxon rank sum test were used to obtain P-value depending on the parametricity of the datasets.

Figure S2

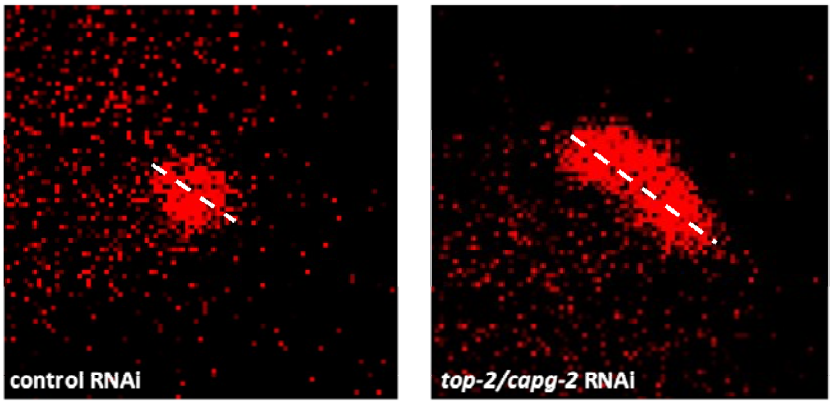

Figure S2: Bivalent length quantification method employed in Figure 6.

Example images of bivalents in -2 oocytes treated with either control or *top-2/capg-2* RNAi are shown. White dashed lines depict the axes that were used for the measurements presented in Figure 6B.

Figure 7

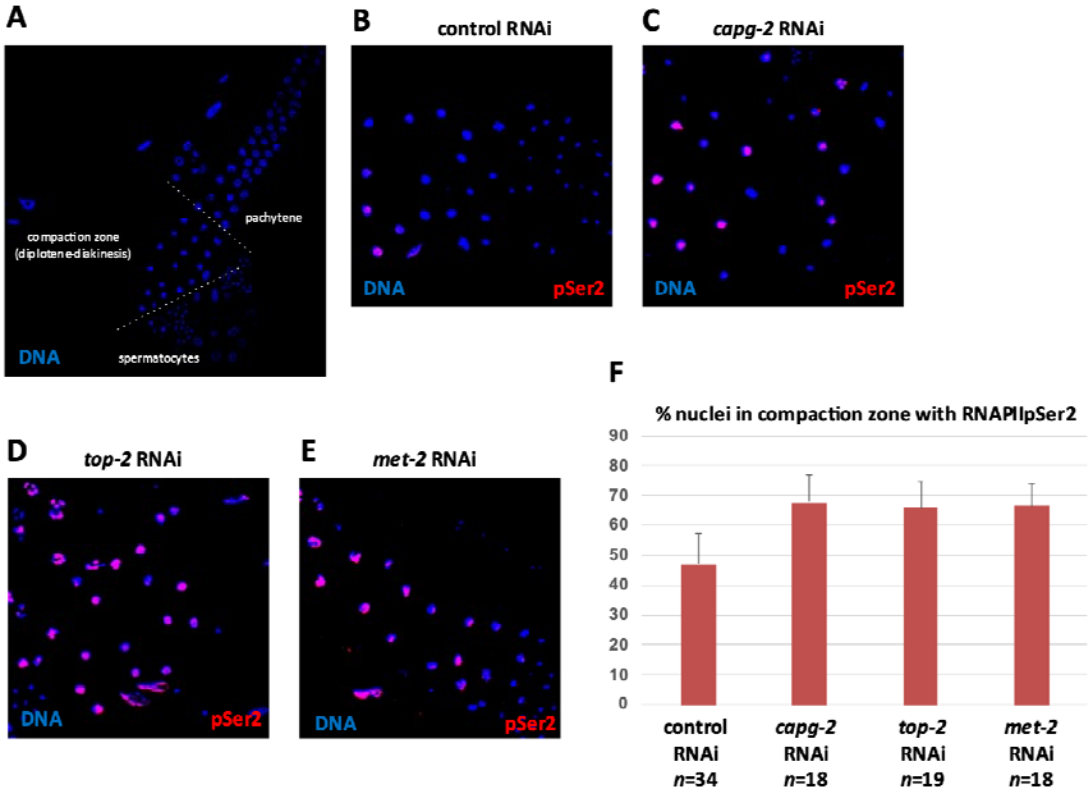
A
compaction zone
(diplotene-diakinesis)
pachytene
spermatocytes
DNA
B
control RNAi
DNA
pSer2
C
capg-2 RNAi
DNA
pSer2
D
top-2 RNAi
DNA
pSer2
E
met-2 RNAi
DNA
pSer2
F
% nuclei in compaction zone with RNAPIIpSer2
90
80
70
60
50
40
30
20
10
0
control RNAi n=34
capg-2 RNAi n=18
top-2 RNAi n=19
met-2 RNAi n=18

Figure 7: TOP-2, condensin II and MET-2 are required for transcriptional repression in spermatocytes.

A. Dissected wild-type male gonads were fixed and stained for DNA (blue). The gonad is divided into three regions based on DNA morphology. The compaction zone, comprised of diplotene and diakinesis spermatocytes, was examined in subsequent experiments.

B. Gonads from male animals treated with control RNAi were fixed and stained for DNA (blue) and RNAPIIpSer2 (red). Representative image of the compaction zone is shown.

C. Gonads from male animals treated with *capg-2* RNAi were fixed and stained for DNA (blue) and RNAPIIpSer2 (red). Representative image of the compaction zone is shown.

D. Gonads from male animals treated with *top-2* RNAi were fixed and stained for DNA (blue) and RNAPIIpSer2 (red). Representative image of the compaction zone is shown.

E. Gonads from male animals treated with *met-2* RNAi were fixed and stained for DNA (blue) and RNAPIIpSer2 (red). Representative image of the compaction zone is shown.

F. Quantification of data presented in panels B-E. Proportion of compaction zone nuclei that are positive for RNAPIIpSer2 signal are presented as percentages. The number of samples analyzed for each condition is shown below. Error bars represent one standard deviation. RNAi depletion of the GCC pathway components results in a significantly increased number of spermatocytes with RNAPIIpSer2 signal in the compaction zone.

Figure 8

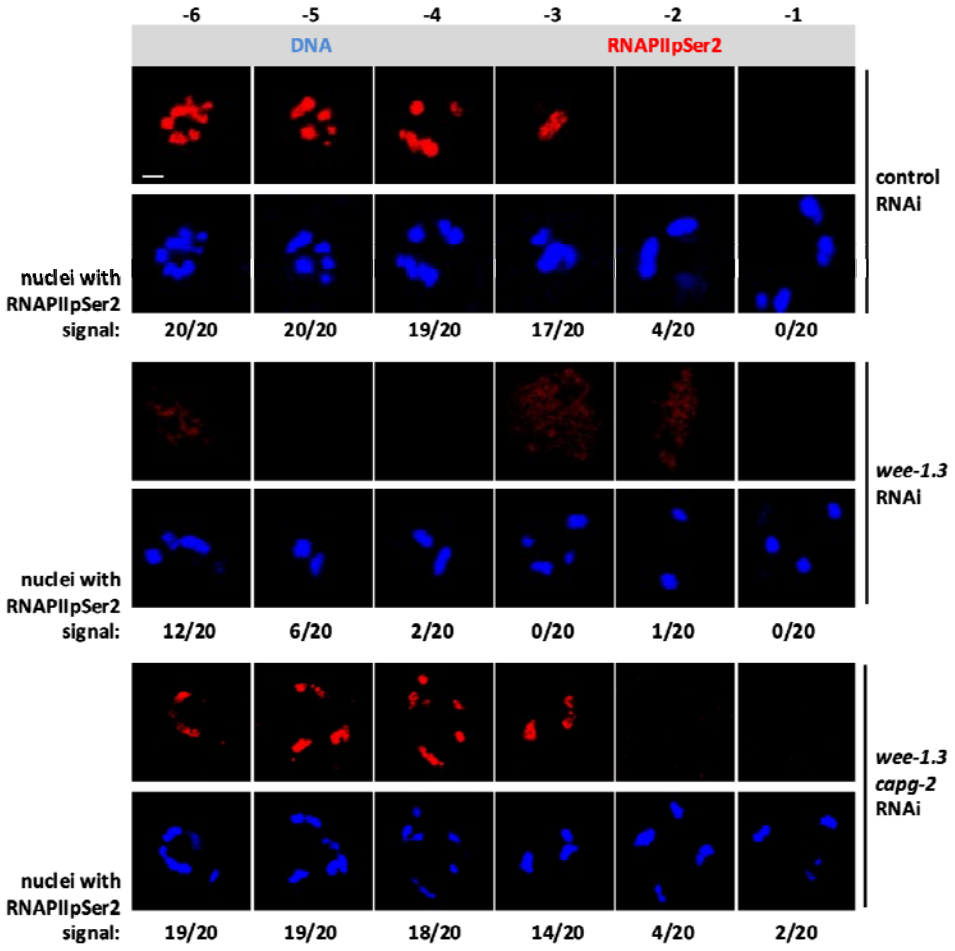
-6
-5
-4
-3
-2
-1
DNA
RNAPIIpSer2
control RNAi
nuclei with RNAPIIpSer2 signal:
20/20
20/20
19/20
17/20
4/20
0/20
wee-1.3 RNAi
nuclei with RNAPIIpSer2 signal:
12/20
6/20
2/20
0/20
1/20
0/20
wee-1.3 capg-2 RNAi
nuclei with RNAPIIpSer2 signal:
19/20
19/20
18/20
14/20
4/20
2/20

Figure 8: Hyperactivation of CDK by the depletion of WEE-1.3 causes unscheduled transcriptional silencing.

N2 animals were treated with either control, *wee-1.3,* or *wee-1.3/capg-2* double RNAi. Gonads were dissected from these animals, were fixed, and stained for DNA (blue) and RNAPIIpSer2 (red). Representative images of the 6 most proximal oocytes are shown for both control and *wee-1.3* RNAi samples. The number of RNAPIIpSer2 positive samples are quantified below each panel. Depletion of WEE-1.3 results in the loss of on-chromatin RNAPIIpSer2 signals in the more distal (-4 to -6 position) oocytes. Additionally, co-depletion using *wee-1.3/capg-2* RNAi reverses the loss of RNAPIIpSer2 signal. Scale bars represent a length of 2 um.